The DEAD Box Protein eIF4A. 1. A Minimal Kinetic and Thermodynamic Framework Reveals Coupled Binding of RNA and Nucleotide†

Jon R. Lorsch and Daniel Herschlag*

Department of Biochemistry, Beckman Center, B400, Stanford University, Stanford, California 94305-5307

Received October 1, 1997; Revised Manuscript Received December 23, 1997

ABSTRACT: eIF4A is the archetypal member of the DEAD box family of proteins and has been proposed to use the energy from ATP hydrolysis to unwind structures in the 5′-untranslated regions of eukaryotic mRNAs during translation initiation. As a step toward understanding the mechanism of action of this class of enzymes, a minimal kinetic and thermodynamic framework for the RNA-activated ATPase function has been established for eIF4A. The enzyme's affinity for ssRNA is modulated by the binding of ATP•-Mg^{2+} and ADP•Mg^{2+}: the affinity of the E•ATP complex for ssRNA is approximately 40-fold higher than that of the E•ADP complex. The enzyme binds its substrates in a random manner; contrary to previous suggestions, neither ATP binding nor hydrolysis is required for binding of single-stranded RNA. The presence or absence of the γ-phosphate on the bound nucleotide acts as a switch that modulates the enzyme's structure and ssRNA affinity. The data presented in this and the following paper in this issue suggest that ATP binding and hydrolysis produce a cycle of conformational and RNA affinity changes in eIF4A. Such cycles may be used by DEAD box proteins to transduce the energy from ATP hydrolysis into physical work, thereby allowing each member of this family to rearrange its RNA or RNA•protein target.

The members of the DEAD box family of proteins are widely distributed in nature and are involved in a variety of cellular processes, including splicing, ribosome biogenesis, RNA degradation, and translation (for reviews, see refs 5 and 6). While genetic analysis has provided much information about what cellular processes certain DEAD box proteins are involved in and, in some cases, even which steps within these processes the enzymes act, little is known at a molecular level about what these proteins do or how they do it.

The DEAD box family and related DEAH and DExH box proteins share sequence similarity with DNA helicases (*7, 8*). This fact, coupled with the observations that these proteins are involved in cellular processes that might be expected to require unwinding of RNA structures (*5, 6*) and that all of the DEAD box proteins that have been studied in vitro have been shown to be RNA-dependent ATPases (for reviews, see refs 5 and 9), led to general models in which these enzymes function as RNA helicases. In several cases, it has been shown that DEAD box proteins are capable of unwinding RNA duplexes in vitro (*10*−*17*), although this activity often requires superstoichiometric concentrations of the protein relative to the RNA substrate.

While DEAD box proteins have become synonymous in the literature with RNA helicases, this term is likely to be misleading because it is unlikely that an enzyme that unwinds RNA structures and a canonical helicase perform precisely the same function. The substrates for canonical helicases are long stretches of a single secondary structure, duplex DNA, and the role of these enzymes is the processive unwinding of such regular structures. In vivo, RNA duplexes are rarely found in contiguous stretches of longer than ∼10 base pairs (*18*), and an enzyme that has the task of disentangling structured RNA molecules would have to deal with a variety of secondary and tertiary structures, not just simple duplexes. Therefore, it is likely that the substrates that a canonical helicase deals with and those that an "RNA helicase" would have to deal with are substantially different.

In addition to disentangling structured RNAs, the DEAD box proteins have other possible functions, including larger scale RNA structural rearrangements and the disruption of RNA−protein or protein−protein contacts (*19*−*21*). It has also been proposed that DEAD box proteins could provide the irreversible step (ATP hydrolysis) required in kinetic proofreading mechanisms (*22*). At present, none of these possible functions can be ruled out for any DEAD box or related protein.

As a starting point in elucidating the molecular mechanism of the DEAD box proteins, we present a detailed kinetic and thermodynamic analysis of the RNA-activated ATPase function of the eukaryotic translation initiation factor eIF4A. eIF4A represents the core DEAD box domain (*5*). The other DEAD box proteins contain a central eIF4A-like domain flanked by N- and/or C-terminal extensions. Thus, insights into how other DEAD box proteins function may be gained by understanding how the core DEAD box domain operates. There has also been a significant amount of initial biochemical characterization of eIF4A on which to build more detailed mechanistic studies.

† This work was supported by a David and Lucile Packard Foundation Fellowship in Science and Engineering to D.H.; J.R.L. was supported by a Damon Runyon−Walter Winchell Foundation Fellowship (DRG 1345).

* Address correspondence to this author. Phone: 650-723-9442. Fax: 650-723-6783. E-mail: herschla@cmgm.stanford.edu.

S0006-2960(97)02430-6 CCC: $15.00
Published on Web 02/06/1998

The role of eIF4A in translation initiation is not fully understood, but the current data regarding its function have been incorporated into a general model for the initiation process. eIF4A has been proposed to be involved in the unwinding of secondary structures in the 5′-untranslated region (UTR[1]) of mRNAs to allow the 40S subunit of the ribosome to bind and scan for the AUG initiator codon (*9*). In mammalian cells, approximately 10% of the ~10 μM eIF4A (*23*) is part of a complex with the cap-binding protein eIF4E and another protein, eIF4G, which appears to serve as a molecular scaffold onto which a number of other protein factors and RNAs assemble (*24*). Collectively these three proteins are called eIF4F. It is commonly accepted that eIF4A is localized to the 5′-end of an mRNA via the cap-binding activity of eIF4E and that it is then able to unwind secondary structures in the 5′-UTR. Another factor, eIF4B, may also be involved in this unwinding process in vivo and is required for the unwinding of RNA duplexes by eIF4A in vitro (*1, 14, 25*−*27*). The ~10-fold higher concentration of eIF4A than eIF4E or eIF4G suggests that eIF4A may also function outside of the eIF4F complex (but see ref 28 for an alternative interpretation).

The kinetic and thermodynamic framework established in this paper demonstrates that the affinity of eIF4A for ssRNA is modulated by the bound nucleotide: the affinity of eIF4A for ssRNA is 40-fold greater when the enzyme is bound to ATP than when it is bound to ADP. This suggests that eIF4A's ATP hydrolysis cycle produces a cycle of RNA affinity changes in the enzyme. These results are extended in the accompanying paper in this issue, which provides evidence that eIF4A undergoes a cycle of ligand-dependent conformational changes. These cycles of thermodynamic and conformational changes, driven by ATP hydrolysis, may be used by eIF4A to rearrange RNA substrates.

EXPERIMENTAL PROCEDURES

Materials. T7 RNA polymerase and IPTG were from United States Biochemicals; ultrapure ATP, poly(U), and poly(A) were purchased from Pharmacia; AMP−PNP, AMP−PCP, ADP, and AMP were from Sigma; ATP-γS was from Boehringer Mannheim; [γ-^{32}P]ATP was purchased from DuPont−NEN; poly(ethyleneimine) (PEI) cellulose plates were from J. T. Baker; nitrocellulose and DEAE cellulose membranes were from Schleicher and Schuell; purified bovine serum albumin was from New England Biolabs.

Oligonucleotides and Transcription of RNA. T7 RNA polymerase runoff transcription was performed after the method of Milligan et al. (*29*). The template strand DNA oligonucleotide for the hairpin dsRNA-I molecule (Chart 1) was 5′-GGA ACC TAG CAG CTT ACG CTG CTA GGT TCC TAT AGT GAG TCG TAT TAC ATA TGC GTG TTA CC-3′. The oligonucleotide used to make the hairpin RNA with the 21-base 5′-single-stranded tail (ss/dsRNA-I; Chart 1) was 5′-GCG ACA GCC TCG CGA ACG AGG CTG TCG CTC TTA ATG ACC TAG AGG TTC CTA TAG TGA GTC GTA TTA CAT ATG CGT GTT ACC-3′. In both cases, the complementary strand was 5′-GGT AAC ACG CAT ATG TAA TAC GAC TCA CTA TAG G-3′. Transcribed RNAs were purified by denaturing poly(acrylamide) gel electrophoresis on 15% poly(acrylamide)/8 M urea gels and eluted into 0.3 M NaCl, followed by ethanol precipitation and resuspension in water. Synthetic RNAs were made on a Millipore Expedite DNA/RNA synthesizer by R. Green in the lab of H. Noller, deprotected with NH_4-OH followed by tetrabutylammonium fluoride (*30*), and purified by anion-exchange high-performance liquid chromatography on a semipreparative column (Dionex) using aqueous ammonium acetate as the eluent.

Chart 1

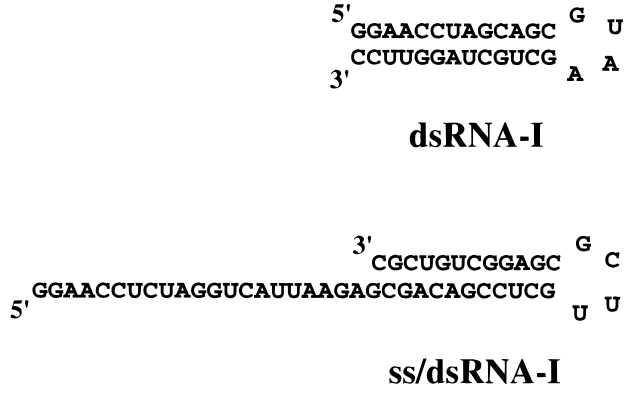

Purification of Recombinant eIF4AI (Mouse) and eIF4B (Human). The overexpression vectors, pET-4A and pET-4B, as well as monoclonal antibodies against the two proteins, were the generous gifts of N. Methot and N. Sonenberg. BL21-DE3 *E. coli* cells harboring the plasmid for overexpression of eIF4A or eIF4B were grown to mid-log phase and induced by the addition of IPTG to a final concentration of 1 mM. The cells were then grown for an additional 2−3 h and were harvested by centrifugation. Cells were resuspended in purification buffer (20 mM Tris−Cl, pH 7.4, 0.1 mM EDTA, 2 mM DTT, 10% glycerol) and lysed by two passes through a French press. The enzymes were purified after the method of Pause and Sonenberg (*14*), with modifications. In the case of eIF4A, a HiTrap Heparin column (Pharmacia) was used after the MonoQ and HiTrap Blue columns. The enzyme eluted from the heparin column at ~150 mM KCl in a linear gradient from 50 to 500 mM KCl in purification buffer. For eIF4B, the lysate was loaded onto an SP sepharose (Pharmacia) column and eluted with a linear gradient of 0.1−1 M KCl in purification buffer. The pooled eIF4B-containing fractions, eluting at ~300 mM KCl, were dialyzed into 50 mM KCl in purification buffer and loaded onto a MonoQ column, which was eluted with a linear gradient of 50 mM−1 M KCl in purification buffer. The eIF4B-containing fractions, which eluted at ~300 mM KCl, were pooled and run over a 60- × 4-cm Sephacryl-100 gel filtration column (Pharmacia) equilibrated in purification buffer with 50 mM KCl. Finally, the eIF4B-containing fractions were applied to the MonoQ column a second time, as described above. Enzymes were stored in purification buffer + 100 mM KCl (referred to as enzyme storage buffer below) at −80 °C. The purified eIF4A was

[1] Abbreviations: UTR, untranslated region; E, enzyme; ss, single-stranded; ds, double-stranded; IPTG, isopropyl 1-thio-β-galactopyranoside; ATP-γS, adenosine-5′-*O*-(3-thiotriphosphate); AMP−PNP, adenylyl imidodiphosphate; AMP−PCP, adenylyl (β,γ-methylene)-diphosphonate; EDTA, ethylenediaminetetraacetate; Tris, tris(hydroxymethyl)aminomethane; HEPES, *N*-(2-hydroxymethyl)piperazine-*N*′-(2-ethanesulfonic acid); MES, 2-(*N*-morpholino)ethanesulfonic acid; DTT, dithiothreitol; SDS, sodium dodecyl sulfate; P_i, inorganic phosphate; PAGE, poly(acrylamide) gel electrophoresis; nt, nucleotides.

≥98% homogeneous and eIF4B was ~90% homogeneous as judged by both coomassie blue and silver staining of SDS−poly(acrylamide) gels.

ATPase Assays. ATPase assays were performed using trace [γ-^{32}P]ATP (≤25 nM) and varying the concentrations of unlabeled ATP. The [γ-^{32}P]ATP was purified prior to use on a 20% nondenaturing poly(acrylamide) gel, eluted in 20 mM Tris−Cl, pH 7.4, and stored at 4 °C. In all cases, ATP, AMP−PNP, AMP−PCP, ATP-γS, and ADP were titrated to pH 7.0 with KOH and were added in stoichiometric amounts with $MgCl_2$ (hereafter, ATP•Mg^{2+}, etc.). AMP−PNP, AMP−PCP, and ATP-γS are supplied as the Li^+ salts; control experiments indicated that LiCl concentrations as high as 100 mM do not inhibit the enzyme relative to its activity with 100 mM KCl (data not shown). No ADP contamination of the AMP−PNP stocks was detectable by TLC, indicating that <5% of the material is ADP. However, 5−10% of the ATP-γS stock was ADP, as judged by TLC. Attempts at further purification were unsuccessful, apparently due to degradation during or following chromatography.

Reaction buffers contained 2.5 mM $MgCl_2$, 1 mM DTT, 1% glycerol, and either 20 mM Tris−Cl, pH 7.4, and 80 mM KCl or 20 mM MES−KOH, pH 6.0, and 10 mM potassium acetate. These conditions are referred to as conditions A and B, respectively, throughout. Reactions (20 μL) were started by the addition of 2 μL of enzyme of the appropriate concentration. The reactions were carried out at constant temperature (37 or 25 °C for conditions A and B, respectively; 37 °C was used for consistency with the conditions used in previous studies of eIF4A), and 2-μL aliquots were quenched at intervals in an equal volume of 25 mM EDTA, pH 8.0. For each reaction, 5−8 time points were taken. The initial rates were measured because product inhibition by ADP prevented the entire reactions from being followed. Time points were spotted onto 6.5-cm strips of PEI−cellulose TLC plates, which were developed first in water and then, after drying, in 1 M LiCl + 0.3 M NaH_2PO_4. The fraction of inorganic phosphate (P_i) in each sample was quantitated using a Molecular Dynamics PhosphorImager. Kinetic analysis was performed using KaleidaGraph software (Abelbeck Software). The fraction of P_i at $t = 0$, typically 1−3%, was subtracted as background.

Dilutions of enzyme were made in enzyme storage buffer (see above). In general, the amount of enzyme added was such that the final concentration should have been 0.25−1.0 μM. However, control experiments showed that in a 20-μL reaction volume, ~100 nM enzyme was lost on the walls of the siliconized polypropylene tubes (Sorenson BioScience). A correction for this loss has been included in the calculations of k_{cat} values and in the nitrocellulose filter-binding experiments. The effects of these corrections were ≤2-fold in all cases. Enzyme concentrations were always below the lowest concentration of substrate used. Background ATPase activity (i.e., in the absence of ssRNA) was found to be ~500-fold below the activity of eIF4A with saturating RNA.

RNA concentrations and thermodynamic constants involving RNA are given in 20-mer units,[2] except where noted, as a U_{20}-mer was found to be approximately the site size for the ssRNA binding site of eIF4A (data not shown and refs 1 and 2).

Steady-State Kinetic Measurements. Steady-state ATPase assays were performed using excess ATP and ssRNA over enzyme (0.25 μM eIF4A). Reactions were followed only during the linear phase: <15% product formation with subsaturating ATP and <1% product formation with saturating ATP. These ranges were used to avoid nonlinearity caused by the strong inhibition from the ADP product. In all cases, multiple turnovers of ATP hydrolysis were monitored, except for measurements in buffer B of the K_m for poly(U) at subsaturating ATP and the K_i's for nucleotides. Because of the low concentration of ATP in these cases, the extent of reaction corresponded to only the first turnover of ATP.

The values of K_m for ATP binding to the free enzyme (E) and the E•ssRNA complex were determined by measuring the velocity of ATP hydrolysis with various concentrations of ATP under conditions of subsaturating ssRNA (K_m with free E) or saturating ssRNA (K_m with E•ssRNA). Analogous experiments were performed to measure the K_m's of ssRNA for E and E•ATP. In each K_m determination, the substrate concentration was varied at least 5-fold above and below the K_m (except that the highest concentration of ATP was 3-fold above its K_m with free E). The other substrate concentration was held constant.

Inhibition constants for nucleotides and P_i were measured by determining the initial velocities of ATP hydrolysis at subsaturating concentrations of ATP in the presence of varying concentrations of inhibitors (0.25 μM eIF4A; inhibitor in excess over enzyme). In each case, eight different inhibitor concentrations were used ranging from at least 5-fold below to at least 5-fold above the K_i. ADP, ATP-γS, and AMP−PNP were shown to be competitive inhibitors in separate experiments: high concentrations of ATP could overcome the inhibitory effects of the nucleotides and restore maximal velocity. The data were fit to the steady-state equation for competitive inhibition using KaleidaGraph.

Pulse−Chase Experiments. All pulse−chase experiments (*31*) were performed under buffer conditions B. To attempt to measure the rate of dissociation of ssRNA from the E•ssRNA and E•ATP•ssRNA complexes, "RNase chase" and dilution chase experiments were performed. In the RNase chase experiments, the RNase degrades any ssRNA that dissociates from eIF4A, thus preventing rebinding. In these experiments, the E•U_{20} complex was formed with 10 μM enzyme and 1.2 μM U_{20} in the presence of [γ-^{32}P]ATP•Mg^{2+}. The ATP hydrolysis reaction (20 μL) was followed for 15 min, then 0, 3, or 13 μM final RNase A was added in the reaction buffer (5 μL), and subsequent reaction was followed for an additional 15 min. In a related set of experiments, [γ-^{32}P]ATP•Mg^{2+} was omitted from the initial reaction mixture and either 1 or 100 μM [γ-^{32}P]ATP•Mg^{2+} (final, after chase) was added with the chase, which again included 0, 3, or 13 μM final RNase A. The rate of ATP hydrolysis was measured after the chases. The results with the 3 and 13 μM RNase chases were the same in all cases.

[2] Except where noted, RNA concentrations and thermodynamic constants involving RNA are given in 20-mer units (i.e., the nucleotide concentration divided by 20). For example, 1 μM poly(U) of ~400 nt would correspond to 1 μM × 400 nt/20 nt = 20 μM 20-mers. These units are used because the site size for ssRNA binding to eIF4A appears to be ~20 nt ((*1, 2*) and J.R.L. and D. H., Unpublished results).

The dilution−chase experiment was performed after the method of Hertel et al. (*32*). The E•poly(U) complex was formed with 10 μM E and 2.5 μM poly(U) and diluted 5-fold into reaction buffer containing 1 μM [γ-^{32}P]ATP•Mg^{2+}, and the rate of ATP hydrolysis was measured. For comparison, poly(U) and enzyme were added separately to the dilution mixture to measure the steady-state rate of ATP hydrolysis under the dilution conditions.

ATP chase experiments were performed to probe the rate of release of ATP from the E•ssRNA•ATP complex. The E•ATP•Mg^{2+} complex was formed using 10 μM eIF4A and 10 μM [γ-^{32}P]ATP•Mg^{2+} (ATP*). This enzyme concentration, however, was still 10-fold below the K_m for ATP•Mg^{2+}, and thus only ~1 μM E•ATP*•Mg^{2+} was expected under these conditions. The reactions were chased by addition of saturating poly(U) (final concentration: 300 μM in 20-mer units) to allow formation of the E•ssRNA•ATP* complex plus 2.5 mM ATP•Mg^{2+} (unlabeled), 250 μM ADP•Mg^{2+} (unlabeled), or a no nucleotide control. Subsequently, hydrolysis of the labeled ATP* was monitored.

As described in the Results and Discussion section, no significant product formation was observed in the pulse−chase experiments with ATP and ssRNA. This is consistent with partitioning of the E•S species such that dissociation of ATP and ssRNA are faster than product formation. There are, however, alternative explanations for this result: (1) No product is observed because the E•S species is not formed under the experimental conditions, or (2) the E•S species formed are nonproductive complexes and therefore cannot form products. The following observations strongly suggest that neither alternative is applicable so that the absence of product formation is indeed indicative of dissociation that is fast relative to product formation. (1) Nitrocellulose filter binding experiments (see Results and Discussion section) provide evidence that an E•ssRNA complex is formed under the eIF4A concentrations used in the pulse−chase experiments. For pulse−chase experiments monitoring ATP release, the amount of E•ATP*•ssRNA complex formed was calculated from the K_m for ATP, assuming that this K_m represents K_d. Several observations described in the Results and Discussion section support the validity of this assumption. (2) The data described in the Results and Discussion section provide no indication of a required order for substrate binding (see "Is substrate binding to eIF4A ordered?").

Nitrocellulose Filter Binding. Filter binding was performed after the method of Wong et al. (*33*) using a Hoeffer 48-well slot blot apparatus. All experiments were done under buffer conditions B. Binding of ssRNA to eIF4A is too weak to allow accurate measurement under buffer conditions A. Nitrocellulose membranes were soaked for 10 min in 0.4 N NaOH, followed by extensive washing with water, soaked for 10 min in 0.5 μM poly(U) (20-mer units) in reaction buffer (to decrease background sticking of poly(U)), washed again with water, and finally soaked in reaction buffer for at least 1 h. DEAE membranes were activated according to the manufacturer's protocol. eIF4A (15 μM) was stored and diluted in 20 mM Tris−Cl, pH 7.4, 80 mM potassium acetate, 2 mM DTT, 0.1 mM EDTA, and 10% glycerol for these experiments. All measurements were performed in triplicate. Binding curves were generated by varying the concentration of eIF4A (typically 10 nM−1 μM) and measuring the fraction of 5′-^{32}P-end-labeled poly(U) (average length ~400 nt; ≤20 nM 20-mers) retained on the nitrocellulose using the PhosphorImager. After the sample was applied to the membranes, it was washed with 200 μL of buffer containing the appropriate ligand. The fraction unbound was measured directly by quantitating the DEAE membrane as well. Background sticking to the nitrocellulose was corrected for as described previously (*33*).

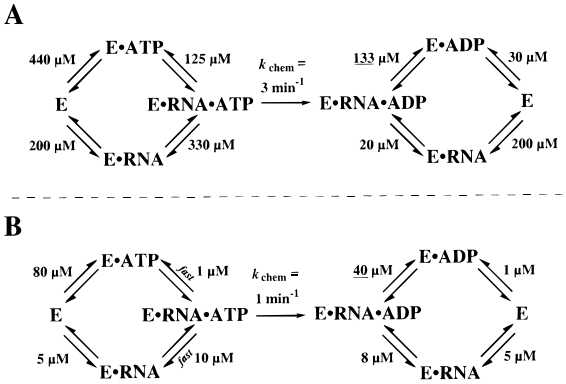

FIGURE 1: Minimal kinetic and thermodynamic schemes for the eIF4A-catalyzed hydrolysis of ATP•Mg^{2+} under buffer conditions A and B. As described in the text, k_{cat} has been assumed to be equal to k_{chem}. The E•ADP•P_i•RNA complex is omitted because of the low affinity of the enzyme for inorganic phosphate and because phosphate release does not appear to be rate-limiting. Underlined values are calculated based on the thermodynamic cycles shown. The overall dissociation constants (the product of dissociation constants along either path from, for example, E + ATP + ssRNA to E•ATP•ssRNA) are not exactly equal to one another due to experimental error.

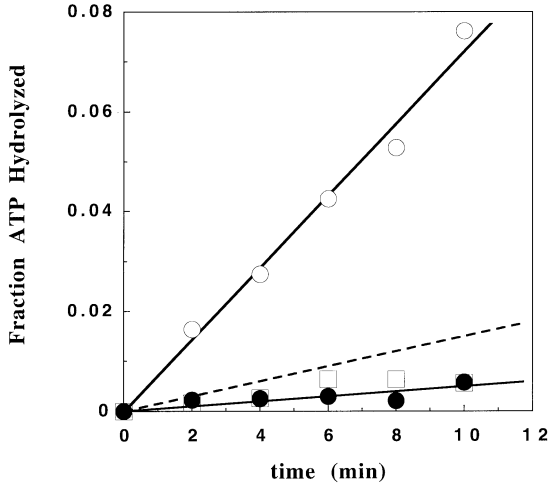

FIGURE 2: Pulse-chase experiments suggest that release of ssRNA is fast. The E•poly(U) complex was formed (2.5 μM poly(U), 10 μM E, buffer B) and then chased by diluting this complex 5-fold in buffer B plus 1 μM [γ-^{32}P]ATP•Mg^{2+} (●). Reactions with no dilution (○) or prediluted 5-fold (□) that were started with 1 μM [γ-^{32}P]ATP•Mg^{2+} are shown for comparison. The curve fit for the undiluted reaction is shown as are the calculated lines for a reaction with a 5-fold lower rate (dashed line) and a 15-fold lower rate (lower solid line).

While this method worked well for the direct measurement of binding of eIF4A to poly(U) (see Figure 4a), it proved difficult to perform competition experiments to measure the affinities for weakly bound ligands such as dsRNA, because it was found that high concentrations of RNA reduced binding of protein to the nitrocellulose membrane. The amount of protein bound to the nitrocellulose membrane was estimated by staining the membrane with coomassie blue

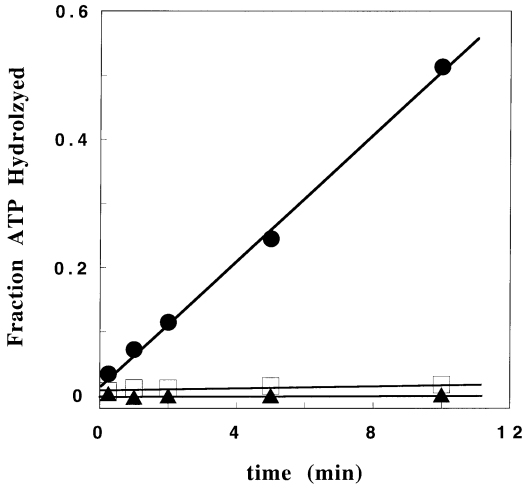

FIGURE 3: Pulse-chase experiment demonstrates release of ATP·Mg^{2+} from the E·ssRNA·ATP·Mg^{2+} complex is fast. E·[γ^{32}P]ATP was formed (10 μM eIF4A, 10 μM γ^{32}P]-ATP·Mg^{2+}) and then diluted into saturating poly(U) alone (250 μM; ●), saturating poly(U) plus 2.5 mM unlabeled ATP·Mg^{2+} (▲), or saturating poly(U) plus 250 μM ADP·Mg^{2+} (□), and the hydrolysis of ATP was followed.

following the experiment. ATP·Mg^{2+}, AMP−PNP·Mg^{2+} and ADP·Mg^{2+} were found to have no effect on the efficiency of retention of eIF4A on the nitrocellulose membrane under the conditions used in the assay. Varying the time of incubation before filtering had no effect on the outcome of the experiments, indicating that the measurements reflect equilibrium binding. The use of a pyruvate kinase/phosphoenol−pyruvate ATP regenerating system to measure the affinity for RNA in the presence of ATP·Mg^{2+} was not possible because it was found that the regenerating system caused the RNA to be retained on the nitrocellulose filter.

The effect of ADP on poly(U) binding was determined with 70 nM eIF4A and varying concentrations of ADP·Mg^{2+}. The fraction of RNA bound at each ADP concentration was measured. The data were fit using eq 1 which was derived from Scheme 1.

$$\text{fraction of RNA bound} = \frac{(xK_{ADP} + [ADP])\left(\frac{K_{ADP}}{[ADP] + K_{ADP}}[E_t]\right)}{[E_t]\left(\frac{K_{ADP}}{[ADP] + K_{ADP}}\right)(xK_{ADP} + [ADP]) + (xK_{RNA}K_{ADP})} \quad (1)$$

In eq 1, K_{ADP} is the dissociation constant for ADP in the absence of RNA, K_{RNA} is the dissociation constant for ssRNA in the absence of ADP, $[E_t]$ is the total enzyme concentration, and x is the coupling factor (i.e., the ratio of the K_d's of the E·ADP complex and free enzyme for RNA; this is equivalent to the ratio of the K_d's for dissociation of ADP from the E·ADP·ssRNA complex and from the E·ADP complex). A value of x greater than 1 indicates anticoupling between ADP·Mg^{2+} and ssRNA, whereas a value less than 1 indicates coupling between the ligands.

UV Cross-Linking. UV cross-linking was performed as described previously (*34*) with the following modifications. The experiments were performed using both buffer conditions A and B. The UV source was a Fotodyne 312-nm hand-held lamp. This wavelength was used because it has been found to efficiently promote cross-linking to 5-bromouridine-substituted RNAs while minimizing photodamage to proteins (*35*). Using a 254-nm UV lamp yielded similar results as those reported here but with reduced efficiency of cross-linking. The 5-bromouridine-substituted RNA (RNA I from ref 34)) was transcribed and purified as described previously (*34*). The plasmid used to transcribe the RNA was the generous gift of N. Methot and N. Sonenberg. Radioactivity was visualized and quantitated using a PhosphorImager (Molecular Dynamics).

Estimation of Errors. In general, rate constants measured on different days usually varied by ≤50% and K_m's and K_d's by ≤2-fold. The exceptions to this were experiments performed with low ssRNA concentrations and either inhibitors or high concentrations of unlabeled ATP·Mg^{2+}. The rate constants obtained from these experiments occasionally varied by as much as 2-fold. Each kinetic and thermodynamic parameter was measured in at least two independent experiments.

RESULTS AND DISCUSSION

Steady-State Kinetics

To begin to elucidate a minimal kinetic and thermodynamic framework for the RNA-activated ATP hydrolysis reaction catalyzed by eIF4A, each of the reaction's steady-state kinetic parameters was measured (Figure 1). Steady-state ATPase assays were performed as described in the Experimental Procedures section. Under the conditions used previously (80 mM KCl, 20 mM Tris−Cl, pH 7.4, 2.5 mM $MgCl_2$, 1 mM DTT, 37 °C; conditions A, hereafter), binding of poly(U) and ATP·Mg^{2+} (Table 1) are both weak, with K_m's of 125 μM (20-mer units[2]) and 330 μM, respectively (results described below strongly suggest that K_m is equal to K_d for both ATP·$Mg^{2+}$and ssRNA). The K_m of 125 μM for poly(U) is in good agreement with the previously reported value of 75 μM determined using eIF4A purified from reticulocyte lysates (*1, 36*). The K_m value for ATP·Mg^{2+}, however, is 3−5-fold higher than the values reported in the literature (*14, 36*−*38*). This modest discrepancy may be the result of differences in experimental procedure or because the strong product inhibition (see below) was not recognized in the previous work. The value of k_{cat} measured herein with poly(U) as an activator is ∼10-fold higher than reported previously (3 vs 0.3 min^{-1} (*14, 36*)). In the previous studies, the value of 0.3 min^{-1} was obtained with saturating ATP but subsaturating poly(U) (25−75 μM) so that the reported value does not represent k_{cat}.

The weak substrate binding observed under the standard assay conditions limited the number of experimental approaches that could be used in the mechanistic studies of eIF4A. Other conditions were therefore sought that might increase the affinity of the enzyme for poly(U) and ATP·Mg^{2+}. Replacing chloride with acetate in the reaction buffer increased binding of poly(U) by an order of magnitude. Lowering the pH of the reaction from 7.4 to 6.0 also increased binding of poly(U) by an order of magnitude. The identity of the buffer was found to have little effect on substrate binding or catalysis. Lowering the temperature from 37 to 25 °C had little effect on substrate affinities but

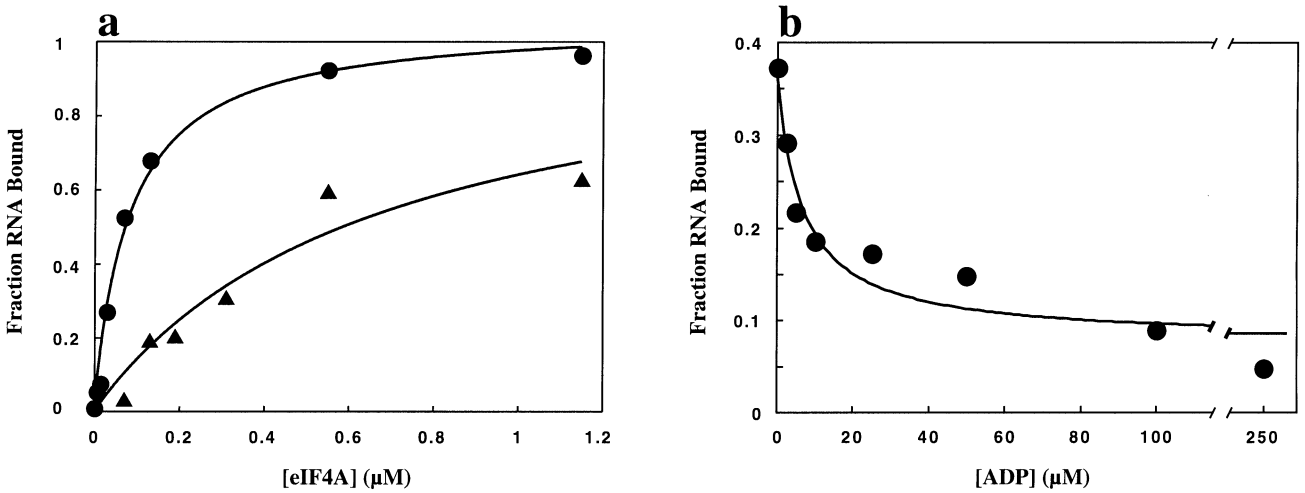

FIGURE 4: Measurement of eIF4A binding to ssRNA using nitrocellulose filter binding. (a) Binding of eIF4A to trace ^{32}P-5′-end-labeled poly(U) in the absence of additional ligands (●) and presence of 250 μM ADP•Mg^{2+} (▲). Each point is the average of three determinations. Curves represent the best-fit lines to the equation (Max[eIF4A])/(K_d + [eIF4A]), where Max is the maximal fraction of poly(U) bound, and give K_d = 0.1 μM in the absence of additional ligands and K_d = 0.7 μM in the presence of ADP•Mg^{2+}; both fits gave end-point values of Max = 1.0, i.e., complete RNA retention at saturating [eIF4A]. The K_d values correspond to K_d's for poly(U) in 20-mer units[2] of 2 and 14 μM, respectively, in the absence of ligand and presence of ADP•Mg^{2+} (K_d's determined as follows: K_d[20-mer units] = K_d^{obsd} × 20 binding sites/poly(U) molecule = 0.1 μM × 20 binding sites/poly(U) = 2 μM in the absence of ADP and K_d[20-mer units] = 0.7 μM × 20 binding sites/poly(U) = 14 μM in the presence of ADP; the value of 20 binding sites/poly(U) molecule is from the average length of the poly(U) of ~400 nt). Three independent measurements of the K_d in the absence of ligands yielded values of 2, 3, and 4 μM. The average value is given in the text. There is more uncertainty in the value of the K_d of the E•ADP complex for RNA than that measured in the absence of ADP•Mg^{2+} because saturation of RNA by eIF4A was not achieved when ADP•Mg^{2+} was present. (b) The fraction of RNA bound in the presence of varying concentrations of ADP•Mg^{2+} (0.07 μM eIF4A and trace ^{32}P-5′-end-labeled poly(U)). Each point is the average of three determinations. The line is a best fit to eq 1 in the Experimental Procedures section. The value of the coupling constant (x) from the fit is 6.9 ± 2. The fit also gave a value for the K_d of the E•ADP complex for RNA of 18 ± 14 μM and a value for the K_d of the E•RNA complex for ADP of 30 ± 15 μM. There are large errors in the K_d values because of the small fraction of RNA bound at the end point, but the value of the coupling constant is relatively insensitive to these uncertainties.

Scheme 1

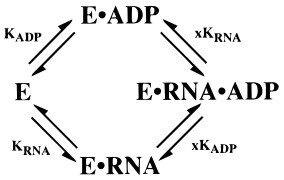

reduced the problem of evaporation during long time courses. Overall, it was found that by lowering the total salt concentration (which stabilizes binding of poly(U) and ATP•Mg^{2+} by ~3-fold and ~4-fold, respectively), replacing chloride with acetate, and lowering the pH of the reaction to 6.0, the affinity of eIF4A for poly(U) was increased by 2 orders of magnitude and the affinity for ATP•Mg^{2+} was increased approximately 10-fold (Table 1). KCl and NaCl have been reported to inhibit the binding of ssRNA to wheat germ eIF4A, although it was not determined whether this effect was due to the cation, anion, or overall ionic strength of the reaction buffer (*2*). The value of k_{cat}/K_m for poly(U), with either saturating or subsaturating ATP•Mg^{2+}, is insensitive to the identity of the cation but is decreased by chloride relative to acetate (data not shown). Chloride also inhibits the binding of ssDNA to RecA, relative to the binding in acetate (*39*).

Table 1: Michaelis and Inhibition Constants for Adenosine and RNA Ligands

	K_m or K_i[a] (μM)			
	buffer A		buffer B	
	E	E•ssRNA	E	E•ssRNA
ATP	440	330	80	10
ADP[b]	27	20	1	8
AMP−PNP		290	25	60
ATP-γS		≥160[c]	≥15[c]	27
AMP−PCP		~5 × 10^3		
P_i[d]		≥5 × 10^4	≥5 × 10^4	>5 × 10^4

	K_m or K_i[a] (μM)			
	buffer A		buffer B	
	E	E•ATP	E	E•ATP
poly(U)	200	125	5	1
poly(A)		115		

[a] Inhibition by ADP, AMP−PNP, and ATP-γS was shown to be competitive in separate experiments (data not shown). [b] Binding of ADP is not affected by the presence of 50 mM P_i, suggesting that binding of ADP and P_i is not coupled or that the K_i for P_i is >0.05 M. [c] These values of K_i for ATP-γS are lower limits because of 5−10% ADP contamination. [d] K_i values for P_i are lower limits because the observed 50% inhibition by 50 mM P_i could result from nonspecific effects.

Presteady-State Kinetics

The overall steady-state parameters governing an enzymatic reaction yield little mechanistic information in and of themselves. Experiments were therefore performed to probe the microscopic rate constants that determine the steady-state parameters. Specifically, the following questions were addressed. (1) What can be learned about the relative rates of the individual reaction steps? (2) What is the affinity of eIF4A for its substrates, and how do the substrate dissociation constants relate to the K_m's? That is, are the Michaelis constants for ssRNA and ATP•Mg^{2+} equal to the dissociation constants? (3) What is the rate-limiting step of the reaction? Such information can provide valuable clues in understanding the mechanism of an enzyme-catalyzed

Scheme 2

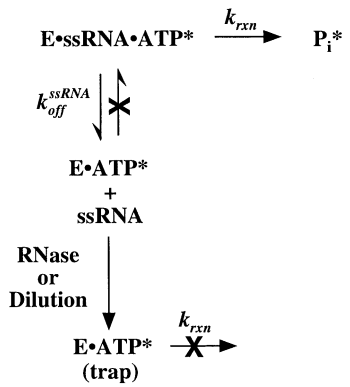

Scheme 3

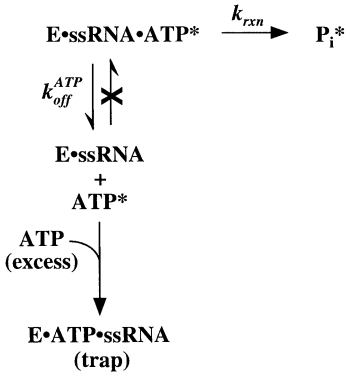

reaction and is crucial for the design and interpretation of future experiments.

Probing the Relative Rates of Individual Steps. Pulse-chase experiments were performed to probe the relative rates of product formation and substrate dissociation (Schemes 2 and 3). In these experiments, the enzyme•substrate complex is formed using high concentrations of enzyme and then "chased" under conditions that prevent rebinding of the substrate of interest once it has dissociated from the enzyme (*31, 40*). If the rate at which the substrate dissociates from the enzyme is slow relative to the rate of the chemical step, then product should be formed during the chase phase of the experiment. However, if the rate of substrate dissociation is fast relative to the chemical step, no product formation will be observed during the chase.

To probe the rate constant for RNA dissociation from eIF4A, the E•U_{20} complex was formed and then chased with either saturating or subsaturating [γ-^{32}P]ATP•Mg^{2+} (ATP*) plus RNase A (Scheme 2). The RNase degrades the U_{20} substrate faster than it can rebind to eIF4A so that dissociation of U_{20} from the E•U_{20} or E•U_{20}•ATP* complex is irreversible (Scheme 2, "trap"). No product was formed in these experiments (data not shown), suggesting that the rate of dissociation of U_{20} from the enzyme is fast relative to the chemical step ($k_{off}^{ssRNA} > k_{rxn}$, Scheme 2). An analogous experiment in which an RNase chase was added during steady-state turnover suggested that dissociation of ssRNA is also faster than product formation during multiple turnover (data not shown).

It is possible that RNase A could degrade U_{20} that is bound to eIF4A, thus making ssRNA dissociation in the above experiments appear faster than it really is. A dilution−chase experiment was therefore performed as an independent test of the rate of RNA dissociation from eIF4A (*32*). In this experiment, the enzyme•ssRNA complex was formed and then diluted 5-fold in reaction buffer and ATP*. If the E•ssRNA complex dissociates faster than the observed rate of the ATPase reaction ($k_{off}^{ssRNA} > k_{rxn}$, Scheme 2), the reaction will be slowed substantially because the concentrations of enzyme and ssRNA are now below the K_d and enzyme must rebind ssRNA before reaction can occur: the ssRNA and enzyme are each diluted 5-fold so that the rate of the reaction would be expected to decrease 15-fold (after Michaelis−Menten equation). However, if ssRNA dissociation is slow relative to the chemical step, the reaction will proceed from the preformed E•ssRNA complex until the complex has had time to dissociate. In this case, the rate of the reaction would decrease only 5-fold upon dilution (rate = k[E•ssRNA][ATP*]). The results of this experiment are shown in Figure 2. The dilution−chase (solid circles) decreases the rate of the reaction ~15-fold (lower solid line) relative to the rate of the undiluted reaction (open circles), as predicted for fast dissociation. In addition, ATP* hydrolysis after the chase was identical to the hydrolysis observed in the control reaction in which the enzyme and ssRNA were added separately under the dilution conditions (solid circles vs open squares). The data of Figure 2 provide additional evidence that the rate of ssRNA dissociation from the E•ATP•ssRNA complex is faster than the rate of product formation.

A pulse−chase experiment was also performed to determine if the rate of ATP dissociation from the E•ATP•ssRNA complex is also fast relative to the rate of product formation (Scheme 3 and Figure 3). In this experiment, 10 μM enzyme was mixed with 10 μM ATP*. These conditions are predicted to be approximately 10-fold below saturation; thus, 1 μM E•ATP* is expected. This E•ATP* complex was diluted 4-fold in reaction buffer containing saturating concentrations of poly(U) and either no chase ligand or a saturating excess of unlabeled ATP or ADP. The large excess of unlabeled ATP or ADP prevents rebinding of labeled ATP once it has dissociated from the enzyme (Scheme 3, "trap"). No burst of product formation was observed with either the ATP or the ADP chase (Figure 3), suggesting that the rate of product formation is at least 5-fold slower than the rate of ATP release from the E•ATP•ssRNA complex ($k_{off}^{ATP} > k_{rxn}$, Scheme 3).

Similar experiments were not performed using buffer conditions A because the large K_m values suggested that significant amounts of the E•S complexes could not be formed under experimentally achievable enzyme concentrations. The large K_m values with buffer conditions A and similar k_{cat} values with the two buffer conditions, however, suggest that substrate dissociation is fast relative to product formation under buffer conditions A as well.

Implications of Fast Substrate Dissociation. The evidence that substrate dissociation from eIF4A is faster than the rate of ATP hydrolysis suggests that the enzyme cannot alone function as a processive helicase. Once an eIF4A molecule has performed one ATP hydrolysis, it will dissociate from its RNA substrate before it can perform a second. It is possible that interaction with other initiation factors alters eIF4A's properties such that it can perform processive unwinding of RNA duplexes. It is also possible that a lack of processivity represents an important mechanistic or

functional difference between eIF4A and the related class of enzymes, the DNA helicases. It is hoped that future mechanistic analyses building upon the initial framework presented herein will determine what mechanistic features are common to eIF4A and processive DNA helicases and what features are unique to each.

What Is the Affinity of eIF4A for Its Substrates, and How Do the Substrate Dissociation Constants Relate to K_m's? To begin to understand the nature of the interactions of eIF4A with its substrates and products, it is necessary to measure the equilibrium dissociation constants (K_d's) for these interactions. Establishing that the values of K_m for the substrates are equal to their K_d's facilitates such an analysis and also provides information about the reaction pathway. Two general situations can cause K_m to be unequal to K_d (*41*). As described below, the data suggest that neither situation holds for eIF4A and that the K_m values for ssRNA and ATP•Mg^{2+} represent dissociation constants under both buffer conditions A and B.

Situation 1: K_m Is Larger than K_d. If the height of the reaction barrier to form products from the enzyme•substrate complex is similar to or lower than the barrier for substrate dissociation from the enzyme, then a preequilibrium will not be established between enzyme and substrate and the measured K_m will be larger than K_d. The pulse−chase experiments described in the previous section provide direct evidence that the rate of substrate release is faster than product formation under buffer conditions B. As outlined at the end of the previous section, the large K_m values suggest that substrate dissociation is fast relative to product formation under buffer conditions A as well. These data strongly suggest that equilibrium is achieved in the substrate binding steps of the reaction catalyzed by eIF4A, and thus, one criterion for K_m being equal to K_d is met.

Situation 2: K_m Is Smaller than K_d. The second situation that can lead to K_m being unequal to K_d is one in which there is a change in the rate-limiting step from, for instance, the chemical step to product release, as the concentration of substrate is increased. In this case, K_m is an underestimate of K_d. If this were true, one would expect to observe a presteady-state burst of product formation when the ATPase assay is performed with high concentrations of enzyme and saturating substrates. Under these conditions, however, no burst is observed under either the A or B buffer conditions (data not shown), suggesting that there is no change in the rate-limiting step with changing substrate concentrations. Furthermore, single-turnover experiments performed with saturating ATP•Mg^{2+} and a saturating excess of eIF4A over ssRNA (buffer B; data not shown) yield values for the rate constant for the conversion of the ternary substrate complex E•ATP•ssRNA to the product complex E•P_i•ADP•ssRNA of $\sim$1 min^{-1}, the same as the measured value of k_{cat}. If a rate-limiting step occurred after chemistry (e.g., dissociation of ADP or P_i), the single-turnover rate constant would be expected to be larger than the multiple turnover rate constant, k_{cat} (see also "What Is the Rate-Limiting Step?" below).

Direct Measurement of ssRNA Affinity. To directly measure the K_d of eIF4A for ssRNA, nitrocellulose filter binding experiments were performed. Several controls were crucial to establish that the results from filter binding experiments represent equilibrium measurements as described in the Experimental Procedures section. Three independent experiments gave an average value of K_d = 3 μM for dissociation of poly(U) from eIF4A (Figure 4a and data not shown; the range of values in three experiments was 2−4 μM). This value is the same, within error, as the K_m of 5 μM (Table 1, buffer conditions B), providing direct support for the above conclusions that the K_ms equal the K_ds. Note that, while filter-binding measurements cannot distinguish between specific binding of RNA and nonspecific binding (i.e., binding to sites other than the active site), the kinetic measurements of ssRNA affinities reflect specific binding, because the ATPase is activated upon ssRNA binding to the active site.

What Is the Rate-Limiting Step of the Reaction? The data outlined above suggest that no rate-limiting step occurs after chemistry and that binding is not the rate-limiting step of the reaction. Thus, in the absence of supporting data for a more complex kinetic mechanism, we adopt a model in which the chemical step is rate-limiting. However, a slow conformational change in the ternary complex that occurs before the chemical step cannot be ruled out, nor can the possibility of rate-limiting release of the first product coupled with an internal equilibrium for ATP hydrolysis that is unfavorable, which would have prevented detection of a fast chemical step in the single-turnover experiments. Immeasurably weak binding of P_i (Table 1) renders the latter possibility unlikely.

Coupled and Anticoupled Binding of Substrates and Products

There is no coupling between the binding of ssRNA and ATP in the ground state under buffer conditions A. The dependencies of the reaction rate on ATP•Mg^{2+} concentration with saturating and subsaturating poly(U) yield K_m's of 330 and 440 μM, respectively, which are the same within error (Figure 5a). As the experiment performed with saturating poly(U) measures ATP•Mg^{2+} binding to the E•ssRNA complex, whereas the experiment performed with subsaturating poly(U) measures binding to the free enzyme (*41*), these experiments suggest that there is no significant difference in the affinity of the free enzyme or the E•ssRNA complex for ATP•Mg^{2+} under these conditions. That is, the binding of the two substrates is not significantly coupled. Similarly, the binding of ADP•Mg^{2+} and ssRNA is also not coupled under these conditions. The K_i's for ADP•Mg^{2+} are 20 and 27 μM with saturating and subsaturating poly(U), respectively (Figure 6a). These data demonstrate that there is no coupling in the ground state between poly(U) and ATP•Mg^{2+} or ADP•Mg^{2+} under buffer conditions A.

In contrast to the absence of ground-state coupling, eIF4A is an ssRNA-activated ATPase, indicating that there is coupling between bound RNA and ATP in the transition state under these conditions. That is, binding of ssRNA stabilizes the transition state for ATP•Mg^{2+} hydrolysis on the enzyme by at least 500-fold or 3.5 kcal/mol (data not shown). This suggests that there are conformational changes in the E•ATP•ssRNA complex associated with attaining the transition state of the reaction, even though these conformational changes may not occur in the ground-state E•ATP•ssRNA complex under buffer conditions A (see also the following paper in this issue).

In contrast to the absence of ground state coupling under buffer conditions A, there is coupling between the binding

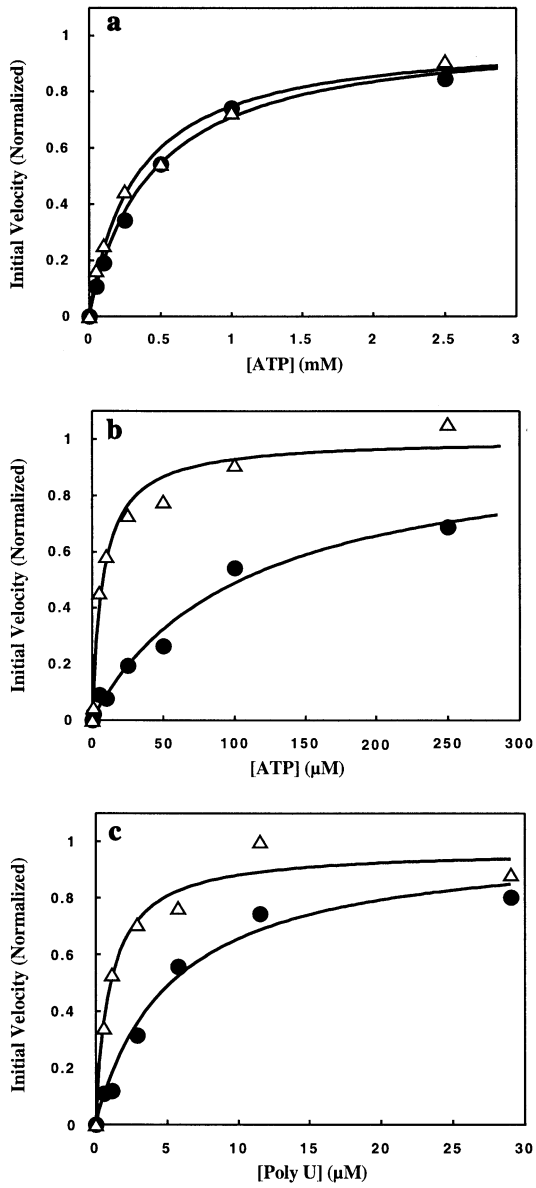

FIGURE 5: Coupling of substrate binding under buffer conditions B but not buffer conditions A. (a) Dependence of ATP hydrolysis rate on concentration of ATP•Mg^{2+} under buffer conditions A with saturating (△) and subsaturating (●) poly(U) (475 and 15 μM, respectively). Measured K_m's are 330 and 440 μM, with saturating and subsaturating poly(U), respectively. (b) Dependence of ATP hydrolysis rate on concentration of ATP•Mg^{2+} under buffer conditions B with saturating (△) and subsaturating (●) poly(U) (30 and 0.6 μM, respectively). Measured K_m's are 10 and 80 μM, with saturating and subsaturating poly(U), respectively. (c) Dependence of ATP hydrolysis rate on the concentration of poly(U) in the presence of saturating (△) and subsaturating (●) ATP•Mg^{2+} yields K_m's of 1 and 5 μM (20-mer units[2]), respectively. Initial velocities are normalized to the V_{max} for each curve for comparison. All curves are best fits to the Michaelis−Menten equation. V_{max} with subsaturating second substrate (ssRNA for a and b; ATP•Mg^{2+} for c) was at least 4-fold lower than that with saturating second substrate in each case, demonstrating that the substrates were indeed subsaturating. For curves with saturating second substrate (△), saturation was demonstrated by showing that the rate did not increase significantly when higher concentrations of the second substrate were used with low or high concentrations of the first substrate (not shown).

of ATP•Mg^{2+} and poly(U) under buffer conditions B. The dependence of the rate of ATP hydrolysis on the concentration of ATP•Mg^{2+} with saturating and subsaturating poly(U) yields values of K_m for ATP•Mg^{2+} of 10 and 80 μM, respectively (Figure 5b). Thus, ATP•Mg^{2+} binds ~10-fold more tightly to the E•ssRNA complex than it does to the free enzyme. Since substrate binding constitutes a thermodynamic cycle (Figure 1), the above data predict, if K_m is equal to K_d, that poly(U) concentration curves at saturating and subsaturating ATP•Mg^{2+} should show the same changes in affinity. Indeed, as shown in Figure 5c, the K_m for poly(U) is ~5-fold lower with saturating ATP•Mg^{2+} than with subsaturating ATP•Mg^{2+} (1 μM vs 5 μM). This confirms that there is coupling between binding of ssRNA and ATP•Mg^{2+} under buffer conditions B.

Poly(U) also affects the binding of ADP•Mg^{2+} under buffer conditions B. With saturating poly(U), the K_i for ADP•Mg^{2+} is 8 μM, nearly the same as it is with buffer conditions A, whereas at subsaturating poly(U) the K_i is approximately an order of magnitude lower, 1 μM (Figure 6b and Table 1). This "anticoupling" observed in the ATPase assays was independently confirmed in nitrocellulose filter binding experiments (Figure 4). The ssRNA affinity is decreased ~7-fold by addition of 250 μM ADP•Mg^{2+} (Figure 4a). Further, Figure 4b shows directly that increasing amounts of added ADP•Mg^{2+} decrease the amount of ssRNA bound to eIF4A. The extent of this effect confirms that the magnitude of the anticoupling is ~7-fold, as described in the figure legend. Therefore, unlike the favorable coupling between ATP•Mg^{2+} and poly(U), poly(U) binding decreases the affinity of the enzyme for ADP•Mg^{2+} (and *vice versa*).

Similar cycles of nucleotide-induced changes in nucleic acid affinity appear to be crucial for the mechanisms of DNA helicases. Such a cycle has been demonstrated for the Rep DNA helicase (*42*) and proposed for the Rho DNA−RNA helicase (*43*−*45*). The coupling between binding of ATP•Mg^{2+} and ssRNA and the anticoupling between binding of ADP•Mg^{2+} and ssRNA reported here for eIF4A could be used by the enzyme to mediate RNA structural rearrangements.

The possibility of coupled binding of ssRNA and AMP−PNP was tested by measuring the K_i for AMP−PNP•Mg^{2+} at saturating and subsaturating poly(U) (Table 1). Unlike the case with ATP, there is no significant increase in nucleotide affinity upon binding of ssRNA, suggesting that this analogue does not interact with the enzyme in precisely the same way that ATP does. This observation and the different behavior of ADP•Mg^{2+} than ATP•Mg^{2+} underscore the importance of the γ-phosphoryl group (see Conclusions section).

Is Substrate Binding To eIF4A Ordered?

It was previously suggested that RNA binds to eIF4A only after ATP is bound (*1, 34, 46*). Because of the potential implications for the mechanism of the enzyme, we reinvestigated the order of binding of eIF4A's substrates and products.

Nitrocellulose filter-binding experiments directly demonstrated that ssRNA can bind to the enzyme in the absence of ATP under buffer conditions B (see *"Direct Measurement of ssRNA Affinity"* above). However, this left open the possibility that binding of ssRNA to eIF4A blocks access to the binding site for ATP. This would necessitate the binding of ATP prior to ssRNA in order to form an active complex. If this were the case, concentrations of ssRNA above the

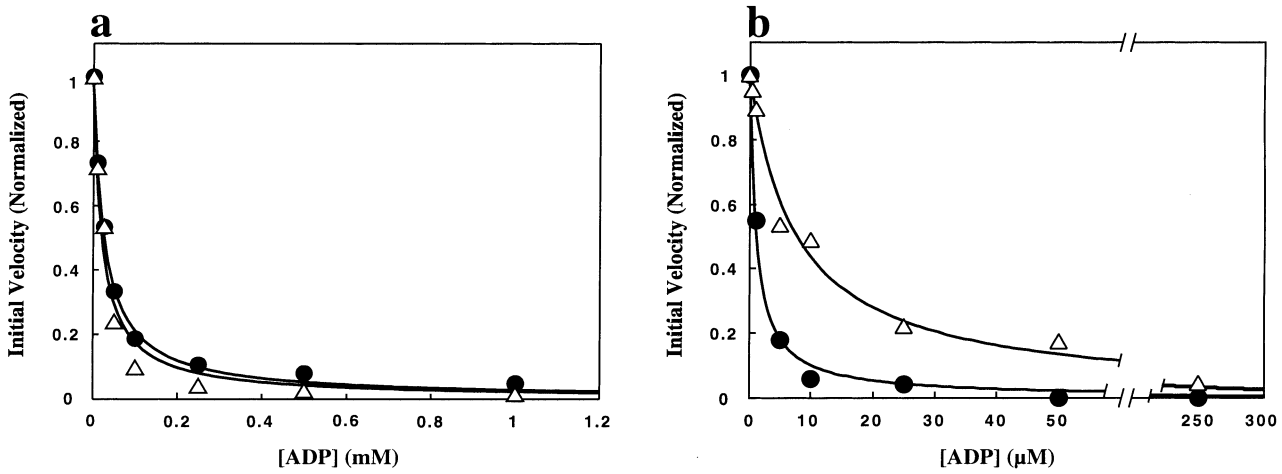

FIGURE 6: Anticoupled binding of ssRNA and ADP·Mg^{2+} with buffer conditions B, but not A. (a) ADP·Mg^{2+} inhibition of ATP hydrolysis was measured with subsaturating ATP·Mg^{2+} (1 μM) and either saturating (△) or subsaturating (●) poly(U) (250 and 15 μM, respectively) using buffer conditions A. The measured K_i's for ADP·Mg^{2+} were 20 and 27 μM, respectively. (b) As in a except under buffer conditions (a) B. K_i's for ADP·Mg^{2+} are 8 and 1 μM with saturating and subsaturating poly(U) (30 and 0.6 μM, respectively), respectively. Curves are nonlinear least-squares fits for competitive inhibition of steady-state turnover. The initial velocities were normalized by dividing by the velocities measured in the absence of ADP·Mg^{2+}.

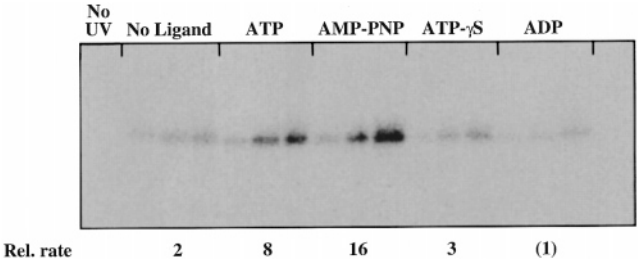

FIGURE 7: UV light-induced cross-linking of 5-Br−U-containing RNA to eIF4A. Internally ^{32}P-labeled RNA was irradiated for 15, 30, and 60 min (left to right) in the absence of ligand or presence of 0.5 mM nucleotide·Mg^{2+} complex. Samples were treated with RNase A and analyzed by SDS−PAGE on a 10% poly(acrylamide) gel. A PhosphorImager scan of such a gel is shown. The rate of cross-linking relative to that seen in the presence of saturating ADP·Mg^{2+}, as determined by quantitation of the radioactivity in the eIF4A−RNA conjugate, is shown under each set of lanes. No band was observed in the absence of UV light ("No UV" lane) or the absence of protein (not shown).

dissociation constant for the E·ssRNA complex could inhibit the reaction by forming nonproductive E·ssRNA complexes. However, no such inhibition is observed (Figure 5c and data not shown), consistent with productive binding of ssRNA in the absence of ATP. Similarly, under buffer conditions A, ssRNA can be cross-linked to eIF4A in the absence of ATP (data not shown), indicating that ssRNA can bind to the free enzyme. There is no inhibition of the ATPase activity at high concentrations of ssRNA (data not shown), consistent with productive binding of ssRNA in the absence of ATP under buffer conditions A.

The converse order of substrate binding, ATP binding only after binding of ssRNA, was also investigated. The ability to UV cross-link ATP to the enzyme in the absence of RNA indicates that ATP can bind to the enzyme before ssRNA (Figure 7 and refs 14 and 34). No inhibition of the reaction by high concentrations of ATP is observed (Figure 5a−c), consistent, as described above, with productive binding of ATP to eIF4A in the absence of ssRNA. These results were obtained under both buffer conditions A and B. Thus, the data suggest that there is no strict order of substrate binding to eIF4A under either buffer condition.

The previous suggestions of ordered binding of ATP and RNA to eIF4A were based on the observations that the binding of eIF4A plus eIF4B to globin mRNA is enhanced by ATP (*1, 46*) and that bromo-U-labeled RNA could only be efficiently UV cross-linked to the enzyme in the presence of ATP, whereas ATP can be cross-linked in the absence of RNA (*34*). Neither of these results, however, establish an order of substrate binding. It is possible that the enhanced binding of globin mRNA in the presence of ATP arose because eIF4A and eIF4B unwound structures within the mRNA, thereby increasing the RNA sites accessible for eIF4A binding. With respect to the cross-linking result, UV cross-linking depends upon the proper alignment of a group in the protein with the reactive group on the ligand. Subtle changes in protein conformation can therefore change this alignment and alter the efficiency of UV cross-linking (*47, 48*). Thus, the absence of UV cross-linking or changes in cross-linking efficiency do not necessarily reflect the extent of, or changes in, ligand binding. The following section presents evidence that the previously observed differences in cross-linking efficiency (*34*) result from changes in protein conformation, rather than ordered binding with a requirement for ATP binding to precede RNA binding.

UV Cross-Linking Experiments Suggest Conformational Changes In eIF4A

It has been reported that ATP, but not the ATP analogue ATP-γS, increases the efficiency of UV cross-linking of bromo-U-labeled RNA to eIF4A relative to what is observed in the absence of nucleotide ligand (*34*). Based on this result, it was suggested that ATP hydrolysis produces an activated state in the enzyme with increased affinity for RNA (*34*). We explored the alternative possibility that the differences in cross-linking efficiency were due to conformational differences between the E·RNA·ATP and E·RNA·ATP-γS complexes rather than a requirement for ATP hydrolysis.

The cross-linking experiments (*34*) were repeated under both the buffer conditions used originally, buffer conditions A, and buffer conditions B. In addition to ATP-γS, a second ATP analogue, AMP−PNP, was also included in our

experiments. We obtained the same results as reported by Pause et al. (*34*) using buffer conditions A (data not shown). Similar results were obtained under buffer conditions B, except the cross-linking was more efficient under these conditions, perhaps due to stronger binding of RNA.

Figure 7 shows the results of the cross-linking experiment using buffer conditions B. The bromo-U-containing RNA is cross-linked relatively efficiently to the enzyme in the presence of saturating ATP·Mg^{2+} but less efficiently in the absence of ligand or the presence of ADP·Mg^{2+} or ATP-γS·Mg^{2+} (4-, 8-, and 3-fold, respectively, relative to saturating ATP·Mg^{2+}). Surprisingly, AMP−PNP·Mg^{2+} produces more efficient UV cross-linking than does ATP·Mg^{2+} (∼2-fold). A similar effect was observed under buffer conditions A (data not shown). The increased cross-linking efficiency of the E·RNA·AMP−PNP complex under both buffer conditions strongly suggests that ATP hydrolysis is not required for RNA binding (*49, 50*).

Under buffer conditions B, the low cross-linking efficiency observed in the absence of ligand or presence of ADP·Mg^{2+} could arise from weaker RNA binding, conformational changes, or a combination of these effects. The ∼10-fold increase in ssRNA binding caused by ATP·Mg^{2+} and the ∼10-fold decrease in ssRNA binding caused by ADP·Mg^{2+} presumably contribute to the inefficient cross-linking with bound ADP·Mg^{2+}. However, AMP−PNP·Mg^{2+} does not enhance the binding of ssRNA, and yet AMP−PNP·Mg^{2+} gives more cross-linking than ATP·Mg^{2+}. This indicates that binding of AMP−PNP·Mg^{2+} to the enzyme stabilizes an enzymatic conformation that gives greater cross-linking efficiency; the absence of an increase in ssRNA binding affinity could be a property of this conformation or could arise because this alternate conformation is not the predominant ground-state species. The decreased cross-linking efficiency of the E·ATP-γS·RNA complex could arise from an alternate enzyme conformation in which the reactive group on the enzyme is not in a favorable position for cross-linking to the reactive group on the RNA or from ADP contamination present in ATP-γS (see the Experimental Procedures section).

No coupling of ligand binding occurs under buffer conditions A (Figure 1), and yet a similar pattern of changes in cross-linking efficiency as those occurring under buffer conditions B is observed (data not shown). Thus, changes in ssRNA binding cannot account for the changes in cross-linking efficiency observed under buffer conditions A. This suggests that the changes in cross-linking efficiency arise from conformational changes in eIF4A complexes under buffer conditions A.

The cross-linking experiments described above suggest that conformational differences and, in some cases, differences in RNA affinity among the various enzyme·nucleotide complexes are responsible for the differences in UV cross-linking efficiency. These results remove the basis for the suggestion that ATP hydrolysis is required for tight binding of RNA. These experiments are also consistent with the data described in the previous section, suggesting that there is no strict order of substrate binding to eIF4A.

Interactions with Single-Stranded RNA

With the exception of the cross-linking experiments, all of the above results were obtained using homopolymeric ssRNA. Because eIF4A presumably needs to operate on the 5′-UTRs of natural mRNAs and because the interactions of the enzyme with homopolymers could be different than its interactions with mixed sequence RNAs, the interaction of heteropolymeric ssRNAs with eIF4A was investigated.

Under buffer conditions B, eIF4A has a ∼4-fold higher K_m for a mixed sequence 21-mer than it does for poly(U): 18 μM for the 21-mer vs 5 μM for poly(U) [20-mer units,[2] subsaturating ATP; Table 1 and data not shown]. The rates of ATP hydrolysis with 5 μM ATP and saturating mixed sequence 21-mer or poly(U) are within 2-fold of each other (0.1 and 0.25 min^{-1}, respectively). Under buffer conditions A, two different mixed sequence ssRNAs (a 135-mer and a 45-mer) stimulated the enzyme's ATPase activity 4−5-fold less effectively than poly(U) with subsaturating ssRNA (subsaturating ATP; K_m and k_{cat} were not determined for these mixed sequence RNAs; data not shown). These results suggest that mixed sequence RNAs bind ∼5-fold more weakly to eIF4A under both buffer conditions A and B. The weaker binding most likely arises from the formation of secondary structures in the mixed sequence RNAs, which decreases the accessible single-stranded binding sites for the enzyme (see next section). The similar binding and ATPase activation suggest, however, that the interactions of eIF4A with mixed sequence ssRNAs are not substantially different than the enzyme's interactions with poly(U).

Does eIF4A Interact With Double-Stranded RNA?

A number of DNA helicases are known to bind double-stranded DNA (*42, 51−53*), and in the case of the Rep helicase, this interaction has been shown to be an integral part of the unwinding mechanism (*42*). To explore the relationship of eIF4A to canonical DNA helicases, the interactions of eIF4A with double-stranded (ds) RNA molecules were examined.

An RNA hairpin molecule (Chart 1, dsRNA-I) did not stimulate the ATPase activity of eIF4A, even at the highest concentrations tested (50 μM dsRNA, buffer conditions B). This result is consistent with the work of Abramson et al., who showed that the ATPase activation provided by poly(U) was decreased by titrating in oligo $(A)_{12-18}$, presumably because poly(U) and oligo A formed duplex regions that did not activate the enzyme (*1*). We could not detect any inhibition of the ssRNA-stimulated ATPase activity of the enzyme by the dsRNA molecule, even with 40 μM dsRNA, at saturating or subsaturating ATP·Mg^{2+} (250 and 1 μM, respectively; data not shown). In these inhibition experiments, subsaturating poly(U) was used so that any inhibition measured would reflect binding to the free enzyme and so that a measured K_i would be equal to the K_d, assuming competitive binding. No inhibition was detected in a similar experiment using saturating ssRNA, providing no indication of a second binding site for dsRNA. As it was possible that dsRNA only binds to the ADP-bound state of the enzyme, we tested to see if ADP inhibition was increased by the presence dsRNA. No change in ADP inhibition was detected in the presence of 20 μM dsRNA (subsaturating poly(U); data not shown).

The above data suggest that dsRNA binds weakly, if at all, to eIF4A. It remained possible, nevertheless, that a second RNA binding site on the enzyme could bind dsRNA

without affecting the enzyme's ATPase activity. Using the nitrocellulose filter-binding assay with enzyme concentrations with which it was possible to detect ~50% binding to a 20-mer ssRNA substrate, no binding was detected to dsRNA-I (buffer conditions B). The possibility that dsRNA binds to a second RNA binding site on the enzyme, but only when ATP•Mg^{2+} or ADP•Mg^{2+} is also bound, is unlikely because no coupling between ATP•Mg^{2+} or ADP•Mg^{2+} and dsRNA binding was detected.

The possibility that the enzyme might interact with the double-strand/single-strand junction of a molecule possessing both double-stranded and single-stranded regions was also investigated. Such a molecule is presumably a better analogue of the RNA substrates that eIF4A would encounter in vivo than are completely single-stranded or double-stranded molecules. At least one DNA helicase, the SV40 large T antigen, recognizes a double-strand/single-strand junction specifically (*54, 55*). With subsaturating ATP•Mg^{2+}, the K_m for ATPase activation by ss/dsRNA-I, a hairpin molecule with a 21-base 5′-single-strand tail (Chart 1), is within 2-fold of that for a molecule consisting of only the 21-mer single-strand region (K_m = 8 and 19 μM, respectively, on a per molecule basis). The value of k_{cat} was also unaffected. Thus, it seems that there are no strong interactions between the enzyme and the ss/ds junction region of this molecule, nor does the ss/ds junction region affect catalysis. We have not yet explored the possibility that eIF4A might interact differently with a forked RNA substrate (i.e., one that has both 5′- and 3′-ssRNA tails on the same side of a duplex region).

The above data suggest that eIF4A does not contain a dsRNA binding site, consistent with its apparent inability to unwind RNA duplexes on its own (see next section). Gibson and Thompson have analyzed the sequences of DEAD box proteins and proposed that a number of these proteins, including RNA helicase A, p68, NPH-II, and vasa, have dsRNA binding sites and that these enzymes should thus function as helicases in the absence of other factors (*56*). More experimental work will be required to test these predictions fully.

Interactions with Other Translation Factors

The proposed mechanisms for duplex DNA unwinding by DNA helicases require multiple DNA binding sites (*45, 57, 58*). DNA helicases meet this requirement by multimerizing (usually as dimers or hexamers (*58*)). Current data, however, suggest that eIF4A is an active ATPase as a monomer (ref 46 and M. Peck, J.R.L., and D.H., Unpublished Results). Therefore, eIF4A may need to associate with another factor that has a binding site for single- or double-stranded RNA in order to unwind RNA duplexes. eIF4B is the most likely candidate to perform such a function. In vitro unwinding assays with eIF4A either require or are strongly stimulated by eIF4B (refs 10, 12, 14, 25, 27 and 34 and M. Marshall, M. Peck, J.R.L., and D.H., Unpublished Results). In vivo, a yeast homologue of eIF4B has been shown to suppress a temperature-sensitive mutation in eIF4A (*59, 60*). Other initiation factors such as eIF4G may also affect the function of eIF4A.

Using eIF4A and eIF4B purified from rabbit reticulocyte lysates, Merrick and co-workers reported that the presence of 0.6 μM eIF4B decreased the K_m of eIF4A for poly(U) by approximately 2 orders of magnitude (*36*). In contrast, we did not observe this effect using the factors expressed in and purified from *E. coli*. Neither the k_{cat} nor the K_m for poly(U) is changed significantly by the presence of 0.5 μM eIF4B (k_{cat} = 4 vs 3 min^{-1} and K_m = 190 vs 125 μM with and without eIF4B, respectively, buffer conditions A; data not shown). The reaction conditions used were nearly identical to those used by Merrick and co-workers, the only difference being the use of Tris herein instead of HEPES. The recombinant eIF4B was shown in separate experiments to support eIF4A-dependent RNA unwinding (data not shown).

An effect of 2 orders of magnitude is unlikely to be due to experimental error. Thus, the difference between the present results and those of Merrick and co-workers could be due instead to the source of the factors. For example, the eIF4B isolated from reticulocyte lysates is modified by phosphorylation, whereas that expressed in and purified from *E. coli* may not be (*61*−*65*). It will be interesting to determine if these or other protein modifications, potential points for the regulation of factor activity, do indeed alter the interactions between these (and other) initiation factors. Since the rabbit reticulocyte lysate eIF4B was only ~80% pure (*66*), another possible explanation for the discrepancy reported here is that the decrease in eIF4A's K_m for poly(U) was caused not by eIF4B but by an unidentified factor in the preparation.

While buffer conditions B do not reflect in vivo salt concentrations or pH,[3] it is possible that these conditions stabilize conformations of eIF4A that are stabilized in vivo by interaction with other factors. It will be interesting to see if such factors, in fact, change the energetics and kinetics of eIF4A's association with its substrates and products. Furthermore, while the energetic couplings reported in this paper are modest, larger couplings may occur under other conditions or in the presence of factors that interact with eIF4A. The ATP•Mg^{2+}- and eIF4B-dependent RNA unwinding activity of eIF4A is maintained under buffer conditions B (M. Marshall, M. Peck, J.R.L., and D.H., Unpublished Results), indicating that cooperation between these two factors in RNA unwinding is not disrupted under the new conditions.

Having established the mechanistic frameworks presented above, it will be possible to determine how interactions with other initiation factors and components of the translational machinery alter the individual binding, catalytic, and conformational steps of the eIF4A-catalyzed ATP hydrolysis reaction. It is expected that this will shed light on the role of eIF4A in translation initiation.

CONCLUSIONS

In contrast to previous proposals (*1, 34, 46*), the binding of substrates to eIF4A is not an ordered process and ATP hydrolysis is not required for tight binding of RNA. The kinetic and thermodynamic framework presented in this paper, however, does provide evidence that eIF4A modulates

[3] Buffer B has a low concentration of acetate, whereas buffer A has chloride. High concentrations of Cl^-, however, are also not present in vivo. Acetate and glutamate are, in general, more biologically relevant anions (*3*). A number of enzymes that utilize nucleic acids are adversely affected by chloride (*4*).

its affinity for single-stranded RNA by sensing whether ATP•Mg^{2+} or ADP•Mg^{2+} is bound in the ATPase active site. This coupling between the binding of nucleotide and ssRNA and the data from the UV cross-linking experiments suggest that interactions between eIF4A and its adenosine phosphate and ssRNA ligands alter the enzyme's structure. As described below, the presence or absence of the γ-phosphate of the bound nucleotide appears to act as a switch that produces some of these structural changes.

The γ-Phosphate as a Switch. ADP•Mg^{2+} binds to both the free enzyme and enzyme•ssRNA complex approximately 10-fold more tightly than ATP•Mg^{2+} under buffer conditions A and binds ~80-fold more tightly to the free enzyme than ATP•Mg^{2+} under buffer conditions B (Table 1). These data suggest that there are unfavorable interactions between the enzyme and either the γ-phosphate of ATP•Mg^{2+} or the Mg^{2+} coordinated to the γ-phosphate. The weak binding of inorganic phosphate is consistent with this suggestion (Table 1). Such unfavorable interactions could be used to cause a conformational change in the enzyme.

AMP−PNP•Mg^{2+}, which differs from ATP•Mg^{2+} in the geometry and chemical nature of the γ-phosphoryl group, does not bind to the enzyme cooperatively with ssRNA under buffer conditions B. This suggests that interactions with the γ-phosphate and its precise alignment in the enzyme's active site are crucial for coupled binding. The differing efficiencies of UV cross-linking of RNA to the E•ATP, E•ADP, E•ATP-γS, and E•AMP−PNP complexes also suggest the importance of the chemical nature of the γ-position of the bound nucleotide for the enzyme's conformation.

Finally, the fact that binding of ATP•Mg^{2+} and ssRNA is coupled under buffer conditions B whereas binding of ADP•Mg^{2+} and ssRNA is anticoupled further suggests that the structure and energetics of the enzyme are modulated via contacts with the γ-phosphate and the Mg^{2+} bound to the β- and γ-phosphates. The observed affinity changes are likely to be the result of conformational differences between the E•ATP and E•ADP complexes and between the E•ATP•ssRNA and E•ADP•ssRNA complexes.

The modulation of energetic coupling and conformational changes by the presence or absence of the γ-phosphate suggests that the ATPase active site of eIF4A may resemble those of other Walker motif-containing NTPases that perform work. Structural analysis of such NTPases has demonstrated the presence of a "γ-phosphate sensor" that alters the structure of these enzymes depending on whether an NTP or NDP is bound (*67, 68*). eIF4A may use a similar mechanism to transduce the energy from ATP hydrolysis into physical work.

Further Implications. The data presented in this and the following paper suggest that ATP binding and hydrolysis produce a cycle of conformational changes and changes in RNA affinity. Nucleotide-dependent cycles of affinity changes for a second substrate are common in enzymes, including DNA helicases (*58*), that use the energy of NTP hydrolysis to perform work. As described in the following paper in this issue, eIF4A (and, perhaps, related DEAD box proteins) may use cycles of affinity and conformational changes in the rearrangement of RNA structures and/or RNA•protein complexes.

In generating new models for the mechanism of eIF4A, it will be necessary to acknowledge that the molecular functions of this and the other DEAD box proteins remain unclear. While this family of enzymes has come to be called RNA helicases, in no case is it certain that a DEAD box protein actually performs this function in vivo. Several observations in this work and elsewhere suggest mechanistic and functional distinctions between eIF4A and canonical helicases. The substrates that a canonical, processive helicase operates on are longer and more regular structures than eIF4A would encounter. All known DNA helicases are multimeric, whereas there is no indication of multimerization of eIF4A. Finally, eIF4A dissociates from ssRNA faster than it hydrolyzes ATP and, thus, is unlikely to function alone as a processive helicase.

It remains to be determined whether the unwinding activity observed in vitro with eIF4A and eIF4B reflects the biological function of these proteins or is a side reaction that arises as the consequence of the enzyme's actual function. The kinetic, thermodynamic, and conformational frameworks presented in this and the following paper in this issue serve as a starting point for determining the mechanistic consequences of eIF4A's interactions with other initiation factors and will help ascertain underlying functional and mechanistic similarities and distinctions between eIF4A and canonical helicases.

Aside from RNA unwinding, other possible roles for the DEAD box proteins cannot be ruled out, such as mediating larger scale RNA structural rearrangements or the disruption or alteration of protein−RNA or protein−protein interactions. Even if the role of eIF4A is to unwind RNA structures, there is no reason at present to believe that all DEAD box proteins perform the same molecular function. It will be exciting in the coming years to see how physical, molecular biological, and genetic techniques can come together to uncover the molecular functions and mechanisms of this important class of enzymes.

ACKNOWLEDGMENT

We are grateful to Nahum Sonenberg for supplying plasmids and monoclonal antibodies to eIF4A and eIF4B and for advice. We thank Alan Sachs, Nathalie Methot, Geeta Narlikar, Matt Peck, and Matt Marshall for advice and discussions and Rachel Green and Harry Noller for synthesizing RNA oligonucleotides and for advice. We thank Alan Sachs and members of our laboratory for comments on the manuscript.

REFERENCES

1. Abramson, R. D., Dever, T. E., Lawson, T. G., Ray, B. K., Thach, R. E., and Merrick, W. C. (1987) *J. Biol. Chem. 262*, 3826−3832.
2. Goss, D. J., Woodley, C. L., and Wahba, A. J. (1987) *Biochemistry 26*, 1551−1556.
3. Alberts, B., Bray, D., Lewis, J., Raff, M., Roberts, K., and Watson, J. D. (1989) *Molecular Biology of the Cell*, 2nd ed.; Garland Publishing: New York.
4. Leirmo, S., Harrison, C., Cayley, D. S., Burgess, R. R., and Record, M. T. (1987) *Biochemistry 26*, 2095−2101.
5. Schmid, S. R., and Linder, P. (1992) *Mol. Microbiol. 6*, 283−292.
6. Wassarman, D. A., and Steitz, J. A. (1991) *Nature 349*, 463−464.
7. Koonin, E. V. (1991) *Nature 352*, 290.
8. Bork, P., and Koonin, E. V. (1993) *Nucleic Acids Res. 21*, 751−752.

9. Merrick, W. C., and Hershey, J. W. B. (1996) *Translational Control* (Hershey, J. W. B., Mathews, M. B., and Sonenberg, N., Eds.), pp 31−69, Cold Spring Harbor Laboratory Press: Cold Spring Harbor, NY.
10. Lawson, T. G., Lee, K. A., Maimone, M. M., Abramson, R. D., Dever, T. E., Merrick, W. C., and Thach, R. E. (1989) *Biochemistry 28*, 4729−4734.
11. Hirling, H., Scheffner, M., Restle, T., and Stahl, H. (1989) *Nature 339*, 562−564.
12. Rozen, F., Edery, I., Meerovitch, K., Dever, T. E., Merrick, W. C., and Sonenberg, N. (1990) *Mol. Cell. Biol. 10*, 1134−1144.
13. Lain, S., Riechman, J. L., and Garcia, J. A. (1990) *Nucleic Acids Res. 18*, 7003−7006.
14. Pause, A., and Sonenberg, N. (1992) *EMBO J. 11*, 2643−2654.
15. Shuman, S. (1993) *J. Biol. Chem. 268*, 11798−11802.
16. Flores-Rozas, H., and Hurwitz, J. (1993) *J. Biol. Chem. 268*, 21372−21383.
17. Jones, P. G., Mitta, M., Kim, Y., Jiang, W., and Inouye, M. (1996) *Proc. Natl. Acad. Sci. U.S.A. 93*, 76−80.
18. Noller, H. F., and Woese, C. F. (1981) *Science 212*, 403−411.
19. Guthrie, C. (1994) *Harvey Lect. 90*, 59−80.
20. O'Day, C. L., Dalbadie-McFarland, G., and Abelson, J. (1996) *J. Biol. Chem. 271*, 33261−33267.
21. Kim, S.-H., and Lin, R.-J. (1996) *Mol. Cell. Biol. 16*, 6810−6819.
22. Burgess, S. M., and Guthrie, C. (1993) *Trends Biochem. Sci. 18*, 381−384.
23. Duncan, R., Milburn, S. C., and Hershey, J. W. (1987) *J. Biol. Chem. 262*, 380−388.
24. Hentze, M. W. (1997) *Science 275*, 500−501.
25. Ray, B. K., Lawson, T. G., Kramer, J. C., Cladaras, M. H., Grifo, J. A., Abramson, R. D., Merrick, W. C., and Thach, R. E. (1985) *J. Biol. Chem. 260*, 7651−7658.
26. Benne, R., and Hershey, J. W. B. (1979) *J. Biol. Chem. 253*, 3078−3087.
27. Methot, N., Pause, A., Hershey, J. W., and Sonenberg, N. (1994) *Mol. Cell. Biol. 14*, 2307−2316.
28. Pause, A., Methot, N., Svitkin, Y., Merrick, W. C., and Sonenberg, N. (1994) *EMBO J. 13*, 1205−1215.
29. Milligan, J. F., Groebe, D. R., Witherell, G. W., and Uhlenbeck, O. C. (1987) *Nucleic Acids Res. 15*, 8783−8798.
30. Scaringe, S. A., Francklyn, C., and Usman, N. (1990) *Nucleic Acids Res. 18*, 5433−5441.
31. Rose, I. A. (1980) *Methods Enzymol. 64*, 47−59.
32. Hertel, K. J., Herschlag, D., and Uhlenbeck, O. C. (1994) *Biochemistry 33*, 3374−3385.
33. Wong, I., Chao, K. L., Bujalowski, W., and Lohman, T. M. (1992) *J. Biol. Chem. 267*, 7596−7610.
34. Pause, A., Methot, N., and Sonenberg, N. (1993) *Mol. Cell. Biol. 13*, 6789−6798.
35. Gott, J. M., Willis, M. C., Koch, T. H., and Uhlenbeck, O. C. (1991) *Biochemistry 30*, 6290−6295.
36. Abramson, R. D., Dever, T. E., and Merrick, W. C. (1988) *J. Biol. Chem. 263*, 6016−6019.
37. Grifo, J. A., Abramson, R. D., Satler, C. A., and Merrick, W. C. (1984) *J. Biol. Chem. 259*, 8648−8654.
38. Blum, S., Schmid, S. R., Pause, A., Buser, P., Linder, P., Sonenberg, N., and Trachsel, H. (1992) *Proc. Natl. Acad. Sci. U.S.A. 89*, 7664−7668.
39. Menetski, J. P., and Kowalczykowski, S. C. (1985) *J. Mol. Biol. 181*, 281−295.
40. Rose, I. A., O'Connell, E. L., Litwin, S., and Tana, J. B. (1974) *J. Biol. Chem. 249*, 5163−5168.
41. Fersht, A. (1985) *Enzyme Structure and Mechanism*, W. H. Freeman and Co., New York.
42. Wong, I., and Lohman, T. M. (1992) *Science 256*, 350−355.
43. Geiselmann, J., and von Hippel, P. H. (1992) *Protein Sci. 1*, 850−860.
44. Geiselmann, J., Yager, T. D., and von Hippel, P. H. (1992) *Protein Sci. 1*, 861−873.
45. Geiselmann, J., Wang, Y., Seifried, S. E., and Hippel, P. H. (1993) *Proc. Natl. Acad. Sci. U.S.A. 90*, 7754−7758.
46. Grifo, J. A., Tahara, S. M., Leis, J. P., Morgan, M. A., Shatkin, A. J., and Merrick, W. C. (1982) *J. Biol. Chem. 257*, 5246−5252.
47. Hockensmith, J. W., Kubasek, W. L., Vorachek, W. R., Evertsz, E. M., and von Hippel, P. H. (1991) *Methods Enzymol. 208*, 211−236.
48. Pashev, I. G., Dimitrov, S. I., and Angelov, D. (1991) *Trends Biochem. Sci. 16*, 323−326.
49. Yount, R. G., Babcock, D., Ballantyne, W., and Ojala, D. (1971) *Biochemistry 10*, 2484−2489.
50. Yount, R. G. (1975) *Adv. Enzymol. Relat. Areas Mol. Biol. 43*, 1−56.
51. Arai, K., and Kornberg, A. (1981) *J. Biol. Chem. 256*, 5253−5259.
52. Das, R. H., Yarranton, G. T., and Gefter, M. L. (1980) *J. Biol. Chem. 255*, 8069−8073.
53. Hingorani, M. M., and Patel, S. S. (1993) *Biochemistry 32*, 12478−12487.
54. Wiekowski, M., Schwarz, M. W., and Stahl, H. (1988) *J. Biol. Chem. 263*, 436−442.
55. Wessel, R., Schweizer, J., and Stahl, H. (1992) *J. Virol. 66*, 804−815.
56. Gibson, T. J., and Thompson, J. D. (1994) *Nucleic Acids Res. 22*, 2552−2556.
57. Hill, T. L., and Tsuchiya, T. (1981) *Proc. Natl. Acad. Sci. U.S.A. 78*, 4796−4800.
58. Lohman, T. M., and Bjornson, K. P. (1996) *Annu. Rev. Biochem. 65*, 169−214.
59. Coppolecchia, R., Buser, P., Stotz, A., and Linder, P. (1993) *EMBO J. 12*, 4005−4011.
60. Altmann, M., Muller, P. P., Wittmer, B., Ruchti, F., Lanker, S., and Trachsel, H. (1993) *EMBO J. 12*, 3997−4003.
61. Duncan, R., and Hershey, J. W. (1984) *J. Biol. Chem. 259*, 11882−11889.
62. Duncan, R., and Hershey, J. W. (1985) *J. Biol. Chem. 260*, 5486-5492.
63. Morley, S. J., and Traugh, J. A. (1989) *J. Biol. Chem. 264*, 2401−2404.
64. Morley, S. J., and Traugh, J. A. (1990) *J. Biol. Chem. 265*, 10611−10616.
65. Tuazon, P. T., Merrick, W. C., and Traugh, J. A. (1989) *J. Biol. Chem. 264*, 2773−2777.
66. Grifo, J. A., Tahara, S. M., Morgan, M. A., Shatkin, A. J., and Merrick, W. C. (1983) *J. Biol. Chem. 258*, 5804−5810.
67. Smith, C. A., and Rayment, I. (1996) *Biophys. J. 70*, 1590−1602.
68. Vale, R. D. (1996) *J. Cell Biol. 135*, 291−302.

BI972430G